PHOTOCATALYTIC DEGRADATION OF SULFAMONOMETHOXINE (SMM) BY $H_3PW_{12}O_{40}/TiO_2$: PREPARATIVE OPTIMIZATION, KINETIC CHARACTERIZATION AND GENERALIZATION STUDY

PU, J. L.[1] – ZHAI, H. Q.[1] – AI, R.[2] – LV, J. D.[1] – BAI, Y. Q.[1] – HE, Z. X.[1] – WANG, M.[1*]

[1]*School of Water Resources and Hydro-electric Engineering, Xi'an University of Technology, Xi'an, Shaanxi 710048, China*

[2]*Besino Environment Ltd, Shanghai 201805, China*

[*]*Corresponding author*
e-mail: wangmin@xaut.edu.cn

(Received 24th Jul 2025; accepted 10th Nov 2025)

Abstract. The pervasive occurrence of antibiotic residues in aquatic systems has emerged as a critical environmental concern worldwide, posing substantial risks to ecological integrity and public health. This investigation presents a strategic approach to combat this issue through the rational design and fabrication of a novel $H_3PW_{12}O_{40}/TiO_2$ composite photocatalyst synthesized via an optimized sol-gel protocol. The systematic optimization of critical preparation parameters, including the PW_{12}/TiO_2 mass ratio (0.25-0.55), calcination temperature (400-600°C), and calcination duration (1-4 hours), were meticulously conducted to maximize photocatalytic efficiency. The optimally engineered catalyst, obtained through calcination at 500°C for 2 hours with a precise PW_{12}/TiO_2 mass ratio of 0.35, demonstrated exceptional performance in degrading sulfamonomethoxine achieving a remarkable degradation rate constant of 0.2121 min^{-1} under UV irradiation. The degradation kinetics adhered rigorously to a pseudo-first-order model, confirming the efficiency of the photocatalytic process. Comprehensive characterization via X-ray diffraction and scanning electron microscopy elucidated the underlying enhancement mechanisms, revealing that PW_{12} doping effectively stabilized the anatase phase, suppressed crystal growth, increased specific surface area, and generated irregular microporous architectures. Furthermore, the composite catalyst exhibited outstanding reusability over multiple cycles and demonstrated broad-spectrum applicability, successfully degrading over 90% of sulfamethazine and ofloxacin within 30 minutes. This study establishes a viable pathway for developing advanced TiO_2-based photocatalytic systems with promising potential for sustainable remediation of antibiotic-contaminated water environments.
Keywords: *antibiotic removal, advanced oxidation processes, anatase stabilization, photocatalytic activity, catalyst reuse*

Introduction

Antibiotic pollution has become an increasingly serious global environmental problem (Hossein and Ripanda, 2025; Shang et al., 2025). Antibiotics such as sulfonamides (Peng et al., 2025), quinolones (He et al., 2025), and tetracyclines (Duong et al., 2024) have been widely detected in rivers (Wu et al., 2025), soil (He, 2025), and sewage treatment plants (Li et al., 2024). They pose a potential threat to ecosystems and public health by accelerating the spread of drug-resistant bacteria. The main sources of these pollutants include agricultural runoff (Damashek et al., 2022), medical and industrial wastewater (Su et al., 2023; Nugraha et al., 2025). However, traditional wastewater treatment processes struggle to remove them effectively, leading to the long-term persistence of antibiotics and their transformation products in the environment.

To address this challenge, advanced oxidation processes (AOPs), especially photocatalytic technology, have become a research hotspot in the field of environmental

http://www.aloki.hu ● ISSN 1589 1623 (Print) ● ISSN1785 0037 (Online)
DOI: http://dx.doi.org/10.15666/aeer/2401_395407

remediation. This is due to their ability to utilize light to generate highly oxidative reactive species (e.g., ·OH and $O_2\cdot^-$) for the complete degradation of recalcitrant organic pollutants (Lu et al., 2013), coupled with mild reaction conditions and no secondary pollution. Among numerous photocatalysts, TiO_2 is highly favored for its low cost, non-toxicity, good chemical stability, and high photocatalytic activity (Yin et al., 2024). However, the practical application of TiO_2 still faces two key challenges: firstly, its relatively wide bandgap limits its utilization of the visible light portion of sunlight (Zhang et al., 2021); secondly, the photogenerated electrons and holes readily recombine rapidly, which severely restricts its overall quantum efficiency (Sinha and Ghosal, 2023; Bertagna Silva and Marques, 2025).

To overcome these limitations, researchers have widely adopted the strategy of constructing composite catalysts. Among them, the composite system of phosphotungstic acid $H_3PW_{12}O_{40}$ and TiO_2 shows significant advantages. $H_3PW_{12}O_{40}$, as a typical Keggin-type heteropoly acid, not only possesses good photochemical stability and strong oxidizing ability itself but can also effectively capture and transfer photogenerated electrons from TiO_2 through its unique interfacial charge transfer effect. This process offers a dual benefit: on one hand, it significantly suppresses the recombination of TiO_2 photogenerated charge carriers, improving quantum efficiency; on the other hand, the introduction of $H_3PW_{12}O_{40}$ can potentially broaden the light response range of TiO_2, thereby enhancing its catalytic activity under visible light (Bahrami et al., 2024).

Based on the above background, this study aims to prepare an $H_3PW_{12}O_{40}/TiO_2$ composite catalyst via the sol-gel method. We systematically optimized key preparation parameters such as the phosphotungstic acid doping amount, calcination temperature, and time to achieve the best photocatalytic degradation performance for sulfamonomethoxine (SMM). Furthermore, this study evaluated the degradation performance of this optimized catalyst against other typical antibiotics (such as sulfamethazine and ofloxacin), aiming to provide new ideas and experimental basis for developing efficient and broad-spectrum antibiotic pollution control technologies.

Materials and methods

Chemicals and reagents

The main reagents used are as follows: tetrabutyl titanate (Sigma-Aldrich, 99%, as titanium source), phosphotungstic acid ($H_3PW_{12}O_{40}$, Aladdin, analytical grade, as dopant), absolute ethanol (Sinopharm Chemical Reagent Co., Ltd., as solvent), glacial acetic acid (Macklin, 99%, as hydrolysis inhibitor), triethanolamine (Macklin, 99%, as complexing agent to stabilize the sol), and sulfamonomethoxine (SMM, Dr. Ehrenstorfer, 99%, as the target pollutant). Deionized water was used in the experiments.

Instruments and equipment

The photocatalytic reaction was carried out in a self-made UV photocatalytic experimental setup (as shown in *Figure 1*). The core light source was a 125 W high-pressure mercury lamp with an emission spectrum range of 200-400 nm. The reactor was a cylindrical quartz glass container, with the reaction liquid level placed parallel to the lamp tube at a fixed distance of 9 cm to ensure uniform illumination. The entire system was placed in a dark box to exclude ambient light interference. During the experiment, an external condenser water circulation system maintained the reaction system at room

http://www.aloki.hu ● ISSN 1589 1623 (Print) ● ISSN1785 0037 (Online)
DOI: http://dx.doi.org/10.15666/aeer/2401_395407

temperature. The catalyst crystal structure was analyzed using an X-ray diffractometer (XRD, Bruker D8 Advance, Cu Kα radiation). The catalyst surface morphology was observed using a scanning electron microscope (SEM, Hitachi SU8010). The concentration of SMM in the solution was determined by high-performance liquid chromatography (HPLC, Agilent 1260).

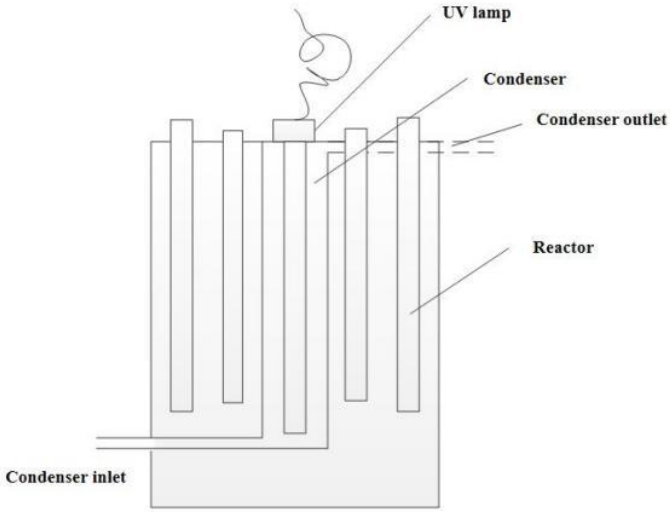

Figure 1. *Ultraviolet photocatalysis experimental setup*

Catalyst preparation

The $H_3PW_{12}O_{40}/TiO_2$ composite (denoted as PW_{12}/TiO_2) was synthesized via the sol-gel method, with the detailed procedure as follows:

Preparation of Solution A: Under room temperature conditions in a 200 mL conical flask with mechanical stirring at 80 rpm, 20 mL of tetrabutyl titanate was slowly added dropwise to 50 mL of absolute ethanol. Subsequently, 3 mL of glacial acetic acid (serving as a hydrolysis inhibitor to prevent excessively rapid hydrolysis of the titanate ester) and 2 mL of triethanolamine (acting as a complexing agent to promote the formation of a stable sol) were added sequentially. The mixture was stirred continuously until homogeneous, yielding a pale yellow transparent Solution A, which was then set aside.

Preparation of Solution B: In another conical flask under identical conditions, 30 mL of absolute ethanol, 5 mL of distilled water, and 2 mL of glacial acetic acid were mixed uniformly. A specific mass of PW_{12}, precisely weighed according to the predetermined PW_{12} to TiO_2 mass ratios (0.25, 0.35, 0.45, and 0.55, respectively), was then added to this mixture. Stirring was continued until the phosphotungstic acid was completely dissolved, resulting in a clear Solution B.

Formation of Sol and Gel: Under stirring at 80 rpm, Solution B was slowly added dropwise to Solution A at a rate of approximately 2 mL/min using a constant-pressure dropping funnel. After the addition was complete, stirring was continued for 1 hour to obtain a uniform transparent sol. This sol was then left to age statically for 2 hours, forming a wet gel.

Drying and Calcination: The resulting gel was placed in a water bath at 100°C and dried for 4 hours, yielding a yellow brittle solid. After grinding, the precursor powder was transferred to a muffle furnace. Under an air atmosphere, the temperature was raised to

http://www.aloki.hu ● ISSN 1589 1623 (Print) ● ISSN1785 0037 (Online)
DOI: http://dx.doi.org/10.15666/aeer/2401_395407

the target values (investigated range: 400-600°C) at a heating rate of 5°C/min and maintained for specific durations (investigated range: 1-4 hours) for calcination. After natural cooling to room temperature, the PW_{12}/TiO_2 catalyst powders with different doping ratios were obtained. Based on preliminary optimization results, unless otherwise specified, the catalysts used in subsequent experiments refer to samples prepared under the optimal conditions (calcination temperature: 500°C, calcination time: 2 hours, PW_{12}/TiO_2 mass ratio: 0.35).

Photocatalytic degradation experiment

The photocatalytic degradation experiments were conducted in the self-made UV photocatalytic reaction setup (identical to *Figure 1*). Initially, 0.1000 g of SMM standard was accurately weighed, dissolved using deionized water, and diluted to a final volume of 100 mL to prepare a stock solution with a concentration of 1.0 g/L. This stock solution was stored at 4°C in the dark. All working solutions for the degradation experiments were prepared by diluting this stock solution to the required concentrations immediately prior to use.

The standard degradation experimental procedure was as follows: A 100 mL working solution of SMM with a concentration of 10 mg/L was prepared in a quartz reaction tube. Subsequently, 100.0 mg of the PW_{12}/TiO_2 catalyst was added, resulting in a final catalyst loading of 1.0 g/L in the reaction system. The magnetic stirrer and air pump were then activated. The continuous introduction of air served both to maintain uniform suspension of the catalyst and to supply the necessary dissolved oxygen for the reaction. Before initiating irradiation, the system was operated in the dark for 30 minutes to ensure adsorption equilibrium of SMM onto the catalyst was reached. Following this adsorption equilibrium period, the 125 W high-pressure mercury lamp (λ = 200-400 nm) was turned on to commence the photocatalytic reaction. The total reaction duration was 30 minutes. During this period, approximately 1 mL samples were withdrawn at predetermined time intervals (0, 5, 10, 15, 20, 25, 30 min). Each collected sample was immediately filtered through a 0.22 μm aqueous syringe filter to completely remove catalyst particles. The resulting clear filtrate was then promptly analyzed by HPLC to determine the residual concentration of SMM.

Concentration determination

The concentration of SMM was determined using an Agilent 1200 high-performance liquid chromatography (HPLC) system. The analysis was performed with a C_{18} column (150 × 4.6 mm, 5 μm) maintained at 35°C. A UV detector set at 270 nm was employed for detection. The mobile phase, consisting of methanol and pure water in a 30:70 volume ratio, was delivered at a flow rate of 1.0 mL/min. The injection volume was 10 μL.

Degradation kinetics analysis

The relative concentration of SMM was represented by the ratio of the concentration at time t to the initial concentration (C_t/C_0), which was used to calculate the degradation efficiency. The pseudo-first-order kinetic model was employed to analyze the effects of three parameters on the SMM degradation rate. The pseudo-first-order kinetic equation is as follows:

$$Ln(C_0/C_t) = kt \quad \text{(Eq.1)}$$

http://www.aloki.hu ● ISSN 1589 1623 (Print) ● ISSN1785 0037 (Online)
DOI: http://dx.doi.org/10.15666/aeer/2401_395407

where C_0 is the initial concentration of SMM at the end of the dark reaction, C_t is the concentration of SMM after irradiation time t, and k is the pseudo-first-order kinetic constant (reaction rate constant). By plotting Ln (C_0/C_t) versus time t, the slope of the resulting straight line gives the reaction rate constant k. The k value directly reflects the intrinsic rate of the photocatalytic reaction, and its maximum value corresponds to the fastest pollutant degradation rate.

Results and discussion

XRD analysis

Phase analysis was conducted on the PW_{12}/TiO_2 catalyst prepared at 500°C and pure TiO_2, with the XRD patterns shown in *Figure 2*. The self-synthesized TiO_2 primarily consisted of the anatase phase, characterized by diffraction peaks at 2θ angles of 25.4°, 37.8°, 48.1°, 53.9°, 55.2°, and 62.8°. These correspond to the (101), (112), (200), (105), (211), and (204) crystal planes of pure anatase TiO_2, respectively, matching the standard PDF card (89-4921). A minor rutile phase diffraction peak was also observed at 2θ = 27.4°, indicating partial transformation of anatase to rutile (Moreno Orea et al., 2025).

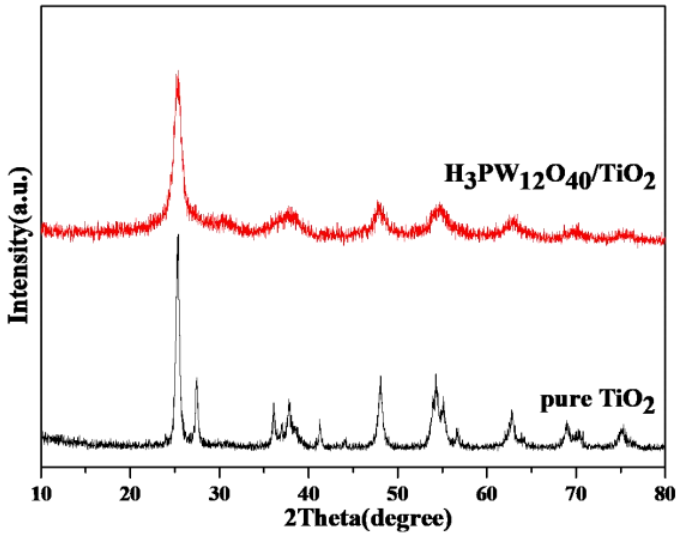

Figure 2. *XRD patterns of PW_{12}/TiO_2 catalyst in comparison with pure TiO_2*

After compositing with PW_{12}, all characteristic peaks corresponded to pure anatase TiO_2, and no rutile phase was detected. This suggests that PW_{12} doping increased the transformation temperature of TiO_2 from anatase to rutile. No characteristic peaks of PW_{12} were observed in the pattern, which could be attributed to the uniform dispersion of PW_{12} within the TiO_2 matrix and the partial substitution of Ti atoms by W atoms in the TiO_2 lattice. The diffraction peaks of the doped sample showed reduced intensity and increased width compared to pure TiO_2, indicating that PW_{12} doping decreased the crystallinity. According to the Scherrer formula ($d = k\lambda/\beta\cos\theta$), the peak broadening implies a smaller crystal size. This demonstrates that PW_{12} doping can inhibit crystal growth, increase the specific surface area, thereby increasing active sites and enhancing both adsorption capacity and photocatalytic performance (Wu et al., 2009).

http://www.aloki.hu ● ISSN 1589 1623 (Print) ● ISSN1785 0037 (Online)
DOI: http://dx.doi.org/10.15666/aeer/2401_395407

SEM analysis

To investigate the effect of PW_{12} doping on the morphology of TiO_2 during the sol-gel preparation process, SEM analysis was performed on both pure TiO_2 and PW_{12}/TiO_2. Representative micrographs obtained at 10,000× magnification are presented in *Figure 3*. Pure TiO_2 exhibited a distinct blocky structure with uneven particle size distribution and severe agglomeration. In contrast, the PW_{12}/TiO_2 composite showed a significantly different morphology, characterized by abundant irregular microporous structures, substantially increased specific surface area, and markedly improved dispersion with reduced agglomeration. This demonstrates that PW_{12} doping effectively prevents the agglomeration of TiO_2 particles during thermal treatment and inhibits TiO_2 grain growth. For the PW_{12}/TiO_2 catalyst, the smaller particle size and larger specific surface area provide more active sites, thereby enhancing the photocatalytic performance. These findings are consistent with the XRD analysis results (Zhang et al., 2021; Jiang et al., 2023).

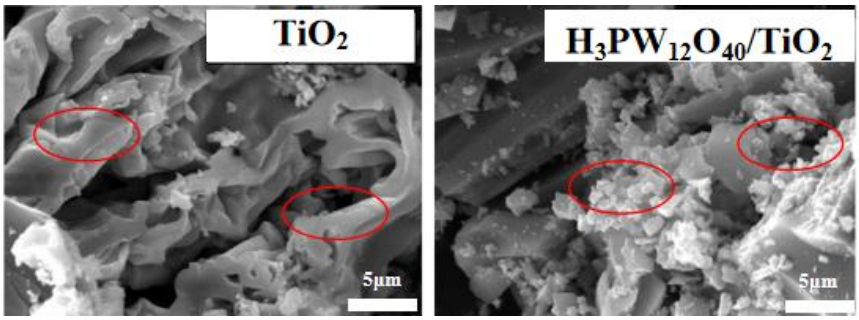

Figure 3. *SEM images of the PW_{12}/TiO_2 catalyst and the TiO_2 catalyst*

The influence of different preparation conditions on the degradation effect

All experiments were conducted with a catalyst dosage of 1.0 g/L and a SMM solution concentration of 10 mg/L. The optimal degradation efficiency of the catalyst under different calcination durations, calcination temperatures, and doping amounts was investigated to determine the preparation conditions for the catalyst with the best performance.

Effect of calcination temperature on the photodegradation of SMM

To investigate the influence of different calcination temperatures on PW_{12}/TiO_2, samples with the same doping amount were calcined at various temperatures for 2 hours and then used to degrade SMM solution under a high-pressure mercury lamp for 30 minutes. The results are shown in *Figure 4a*. Analysis reveals that PW_{12}/TiO_2 calcined at 500°C exhibited the relatively best photocatalytic activity. When the calcination temperature was either higher or lower than 500°C, the catalytic activity of PW_{12}/TiO_2 towards SMM decreased. For composites with the same doping amount, their photocatalytic activity is primarily influenced by the intrinsic properties of TiO_2, such as particle size, crystal structure, and surface composition. At the calcination temperature of 500°C, the anatase characteristic XRD peaks of TiO_2 were relatively distinct. Excessively low calcination temperatures resulted in incomplete crystallization of TiO_2 and a lower content of the anatase phase, leading to poorer catalytic performance. Conversely,

http://www.aloki.hu ● ISSN 1589 1623 (Print) ● ISSN1785 0037 (Online)
DOI: http://dx.doi.org/10.15666/aeer/2401_395407

excessively high temperatures promoted the formation of some rutile-phase TiO_2 in the catalyst, thereby reducing the photocatalytic activity of PW_{12}/TiO_2 (Ma et al., 2017; Synowiec et al., 2023).

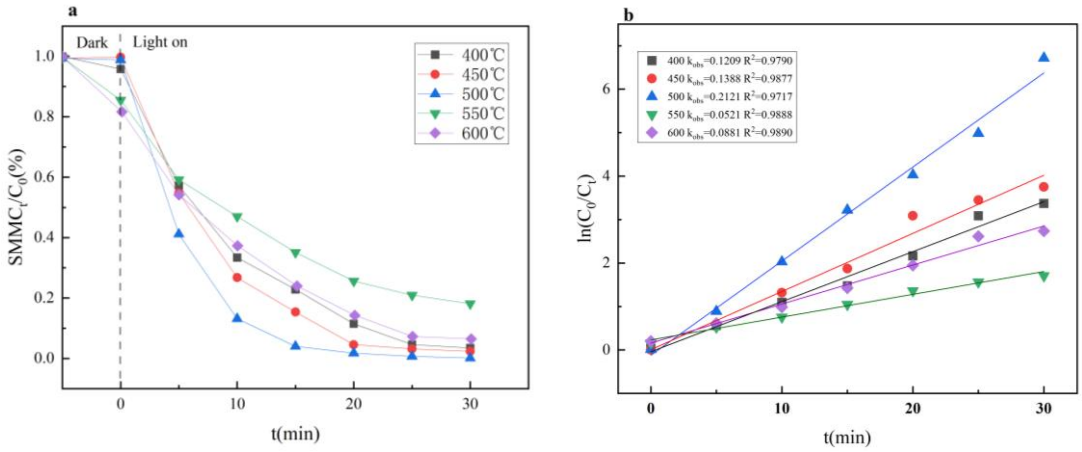

Figure 4. *Effect of calcination temperature on degradation efficiency and the pseudo-first-order kinetics model*

As shown in *Figure 4b* and *Table 1*, the plots of $Ln(C_0/C_t)$ versus time for SMM degradation under the experimental conditions all exhibited well-fitted linear relationships, with determination coefficients (R^2) exceeding 0.9. This demonstrates that the pseudo-first-order kinetic model accurately describes the photocatalytic degradation process of SMM by PW_{12}/TiO_2. The maximum rate constant k of 0.2121 min^{-1} was achieved at the calcination temperature of 500°C, indicating optimal degradation efficiency at this condition. Therefore, 500°C was identified as the optimal calcination temperature for the material.

Table 1. *Parameters of the pseudo-first-order kinetics model at different calcination temperatures*

Influencing Parameters	Reaction Conditions	Reaction Equations	R^2	K (min^{-1})
Calcination Temperature (°C)	400	y=0.1209x-0.0913	0.9790	0.1209
	450	y=0.1388x-0.0358	0.9877	0.1388
	500	y=0.2121x-0.0481	0.9717	0.2121
	550	y=0.0521x+0.2265	0.9888	0.0521
	600	y=0.0881x+0.1677	0.9890	0.0881

Effect of calcination time on the photodegradation of SMM

Effect of calcination time on the photodegradation of SMM

Using a fixed calcination temperature of 500°C, PW_{12}/TiO_2 samples with identical doping amounts were calcined for different durations and subsequently used to degrade SMM solution under a high-pressure mercury lamp for 30 minutes, to investigate the influence of calcination time on degradation efficiency. The results are presented in *Figure 5*.

http://www.aloki.hu ● ISSN 1589 1623 (Print) ● ISSN1785 0037 (Online)
DOI: http://dx.doi.org/10.15666/aeer/2401_395407

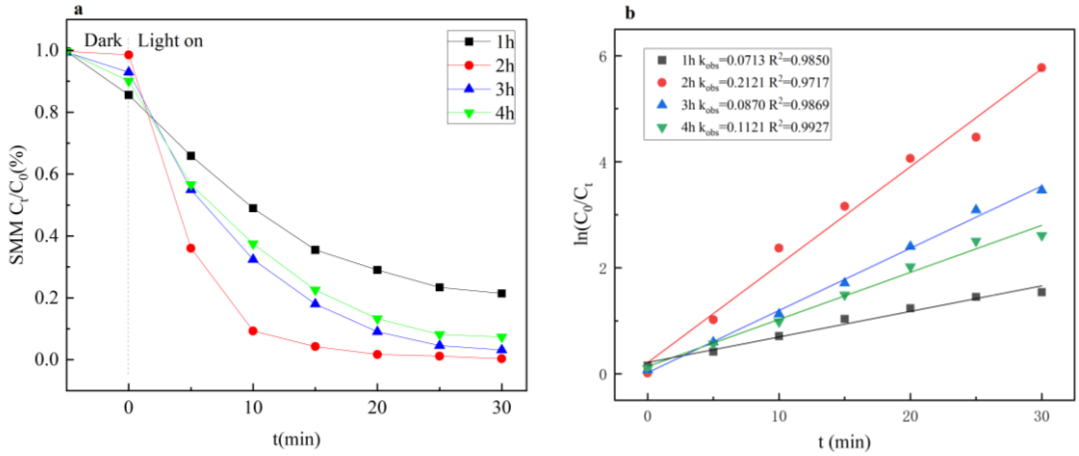

Figure 5. *Effect of calcination time on degradation efficiency and the pseudo-first-order kinetics model*

Using 2 hours as the demarcation point, the photocatalytic activity of the samples increased significantly with extended heat treatment time during the first two hours of calcination. The catalyst calcined for 2 hours exhibited the highest activity. However, when the calcination time exceeded 2 hours, the catalyst activity showed a declining trend. This is because when the calcination time at the same temperature is too short, TiO_2 crystallization is incomplete, resulting in a lower proportion of the anatase phase. Conversely, excessively long calcination times promote the gradual transformation to the rutile phase TiO_2, thereby leading to reduced catalytic activity (O'Byrne et al., 2024).

As shown in *Figure 5b* and *Table 2*, the reaction process follows the pseudo-first-order kinetics model, with the rate constant k reaching a maximum value of 0.2121 min^{-1} at 2 hours. Therefore, 2 hours was selected as the optimal calcination time.

Table 2. *Parameters of the pseudo-first-order kinetics model at different calcination times*

Influencing Parameters	Reaction Conditions	Reaction Equations	R^2	K (min^{-1})
Calcination Time (h)	1	y=0.0713x+0.1630	0.9850	0.0713
	2	y=0.2121x-0.0481	0.9717	0.2121
	3	y=0.087x+0.1429	0.9869	0.0870
	4	y=0.1121x+0.0483	0.9927	0.1121

Effect of PW_{12} loading amount on the photocatalytic degradation of SMM

To investigate the influence of different doping amounts on the degradation efficiency, composite catalysts with varying PW_{12} loadings were prepared, calcined at 500°C for 2 hours, and subsequently used to degrade SMM solution under a high-pressure mercury lamp for 30 minutes. The results are shown in *Figure 6*.

When the mass ratio of PW_{12} to TiO_2 was less than 0.35, the photocatalytic performance gradually improved with increasing phosphotungstic acid doping. However, when the mass ratio exceeded 0.35, the photocatalytic activity of PW_{12}/TiO_2 decreased instead, indicating that the phosphotungstic acid loading significantly affects the photocatalytic activity of TiO_2. This is attributed to the fact that PW_{12} loading modifies

http://www.aloki.hu ● ISSN 1589 1623 (Print) ● ISSN1785 0037 (Online)
DOI: http://dx.doi.org/10.15666/aeer/2401_395407

the surface acidity of TiO_2 and increases the number of surface active sites, thereby enhancing photocatalytic performance. However, when the PW_{12} loading becomes excessive, the surplus $(PW_{12}O_{40})^{3-}$ anions disrupt the colloidal balance of TiO_2, leading to decreased sol stability, and causing precipitation and agglomeration, which reduces the effective surface area of TiO_2 (Chakraborty and Weinstock, 2019), consequently diminishing the degradation performance.

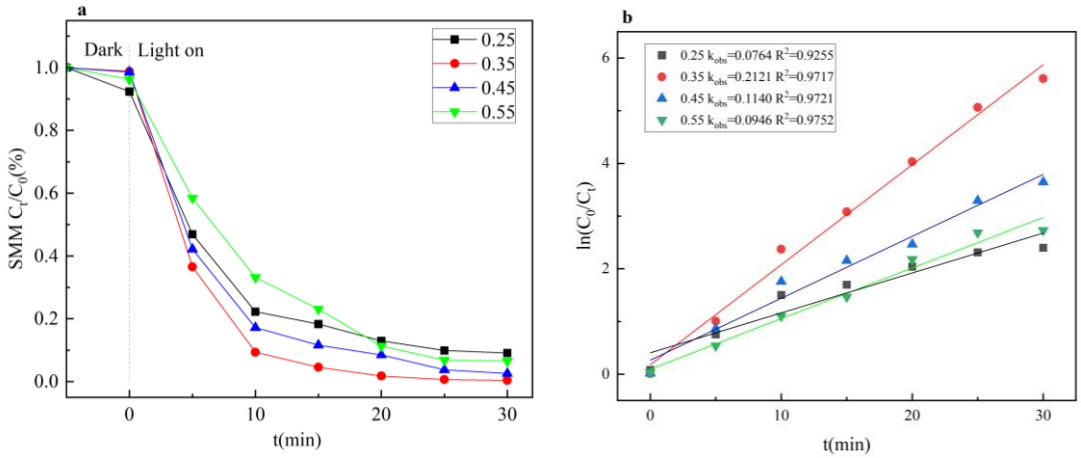

Figure 6. *Effect of doping ratio on degradation efficiency and the pseudo-first-order kinetics model*

As shown in *Figure 6b* and *Table 3*, the reaction process follows the pseudo-first-order kinetics model. The maximum rate constant k of 0.2121 min^{-1} is achieved at a PW_{12}/TiO_2 ratio of 0.35, with all R^2 values exceeding 0.9, indicating that this model satisfactorily describes the degradation process. Therefore, the doping ratio of 0.35 was determined to be the optimal condition.

Table 3. *Parameters of the pseudo-first-order kinetics model at different doping ratios*

Influencing Parameters	Reaction Conditions	Reaction Equations	R^2	K (min^{-1})
Doping Ratio	0.25	y=0.0764x+0.399	0.9255	0.0764
	0.35	y=0.2121x-0.0481	0.9717	0.2121
	0.45	y=0.1140x+0.2795	0.9721	0.1140
	0.55	y=0.0946x+0.1002	0.9752	0.0946

Catalyst reuse performance

Following the optimization of preparation conditions, the catalyst synthesized under optimal parameters (calcination temperature 500°C, calcination time 2 hours, PW_{12}/TiO_2 mass ratio 0.35) was subjected to cyclic degradation tests for SMM. After each experiment, the catalyst was sequentially washed with water, rinsed with methanol, and dried before being reused in the next cycle. The degradation efficiencies recorded were 98.39%, 92.80%, 73.62%, 70.53%, and 67.77% for consecutive cycles. The degradation efficiency remained above 90% during the first and second cycles, indicating excellent structural robustness and sustained TiO_2 photocatalytic activity of the catalyst, which

http://www.aloki.hu ● ISSN 1589 1623 (Print) ● ISSN1785 0037 (Online)
DOI: http://dx.doi.org/10.15666/aeer/2401_395407

facilitates the recovery of active sites and prevents surface contamination (Maharathi and Lo, 2025).

Although a noticeable decline in degradation performance occurred from the third cycle onward, the efficiency still remained above 70%, and approached approximately 70% even at the fifth cycle. This demonstrates good reusability of the catalyst, suggesting its suitability for practical applications. The decrease in degradation efficiency can be attributed to several factors. While the sol-gel method helps immobilize PW_{12} within the TiO_2 matrix, partial leaching of PW_{12} from the catalyst surface may still occur during repeated liquid-phase reactions and washing procedures, leading to a reduction in effective interfacial charge transfer sites. Concurrently, certain organic intermediates generated during SMM degradation may strongly adsorb onto the active sites or within the micropores of the catalyst, forming an inactive overlayer and consequently resulting in the observed decline in degradation efficiency (*Figure 7*).

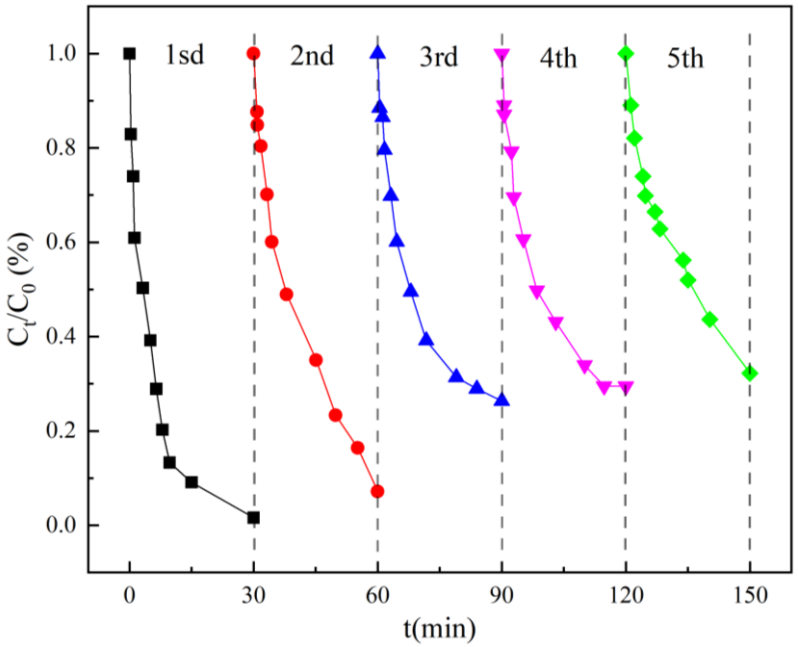

Figure 7. *Catalyst reuse performance curve*

Degradation of other antibiotics by PW_{12}/TiO_2

To evaluate the versatility of the prepared catalyst, photocatalytic degradation experiments were conducted on two other typical antibiotics under identical conditions. The results are shown in *Figure 8*. It was found that the catalyst achieved degradation efficiencies exceeding 90% for both sulfamethazine (SM2) and ofloxacin (OFX) within 30 minutes, demonstrating its good performance and broad-spectrum applicability.

However, several challenges remain to be addressed for the practical application of this technology. In complex real water matrices, such as medical wastewater and aquaculture effluent, the presence of natural organic matter, anions, and suspended solids may compete with target pollutants for active sites or reactive radicals. This competitive inhibition, along with potential light shielding effects, could significantly reduce the degradation efficiency, presenting a major obstacle for scaling up this technology to practical applications.

http://www.aloki.hu ● ISSN 1589 1623 (Print) ● ISSN1785 0037 (Online)
DOI: http://dx.doi.org/10.15666/aeer/2401_395407

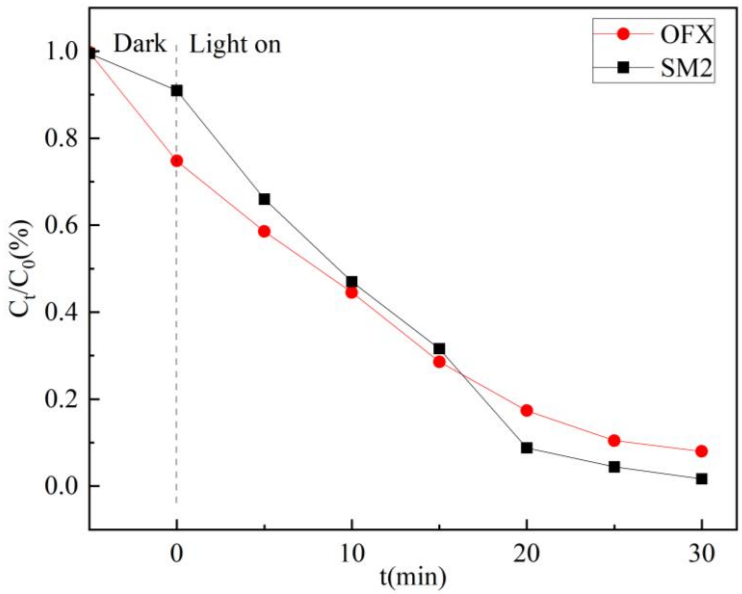

Figure 8. *Degradation curves of the two antibiotics*

Conclusion

This study successfully prepared a PW_{12}/TiO_2 composite photocatalyst via the sol-gel method and systematically evaluated its performance in degrading SMM and other antibiotics. The results demonstrate that PW_{12} doping significantly modulated the microstructure, not only stabilizing the highly active anatase phase and reducing crystal size but also creating abundant micropores, thereby collectively enhancing the catalyst's adsorption capacity and photocatalytic activity.

Through optimization of preparation parameters, the optimal catalyst performance was achieved under the conditions of a calcination temperature of 500°C, calcination time of 2 hours, and PW_{12}/TiO_2 mass ratio of 0.35. The degradation of SMM followed the pseudo-first-order kinetic model with a high-rate constant of 0.2121 min^{-1}. Furthermore, the catalyst exhibited degradation efficiencies exceeding 90% for both SM2 and OFX, demonstrating its potential for broad-spectrum antibiotic degradation. Cycling tests further confirmed the catalyst's good reusability, indicating its fundamental suitability for practical application.

Acknowledgements. This research did not receive any specific grant from funding agencies in the public, commercial, or not-for-profit sectors.

REFERENCES

[1] Bahrami, S., Ahmadpour, A., Rohani Bastami, T., Ayati, A., Mirzaei, S. (2024): Comparative study of metal nanoparticles anchored TiO_2 using polyoxometalate intermediate in photodegradation of azo dye pollutant in aquatic environments. – Inorganic Chemistry Communications 160: 111986. https://doi.org/10.1016/j.inoche.2023.111986.

[2] Bertagna Silva, D., Marques, A. C. (2025): TiO_2-based photocatalytic degradation of microplastics in water: Current status, challenges and future perspectives. – Journal of Water Process Engineering 72: 107465. https://doi.org/10.1016/j.jwpe.2025.107465.

http://www.aloki.hu ● ISSN 1589 1623 (Print) ● ISSN1785 0037 (Online)
DOI: http://dx.doi.org/10.15666/aeer/2401_395407

[3] Chakraborty, B., Weinstock, I. A. (2019): Water-soluble titanium-oxides: Complexes, clusters and nanocrystals. – Coordination Chemistry Reviews 382: 85-102. https://doi.org/10.1016/j.ccr.2018.11.011.

[4] Damashek, J., Westrich, J. R., McDonald, J. M. B., Teachey, M. E., Jackson, C. R., Frye, J. G., Lipp, E. K., Capps, K. A., Ottesen, E. A. (2022): Non-point source fecal contamination from aging wastewater infrastructure is a primary driver of antibiotic resistance in surface waters. – Water Research 222: 118853. https://doi.org/10.1016/j.watres.2022.118853.

[5] Duong, L. T. K., Nguyen, T. T. T., Tran, T. V. (2024): Combined pollution of tetracyclines and microplastics in the aquatic environment: Insights into the occurrence, interaction mechanisms and effects. – Environmental Research 263: 120223. https://doi.org/10.1016/j.envres.2024.120223.

[6] He, J. H. (2025): Antibiotics pollution in cropland and crops: A comprehensive review. – Advanced Agrochem, In Press, Corrected Proof. https://doi.org/10.1016/j.aac.2025.05.002.

[7] He, L. X., He, L., Tang, Y., Qiao, L., Xu, M., Zhou, Z., Bai, H., Zhang, M., Ying, G. (2025): Deciphering spread of quinolone resistance in mariculture ponds: Cross-species and cross-environment transmission of resistome. – Journal of Hazardous Materials 487: 137198. https://doi.org/10.1016/j.jhazmat.2025.137198.

[8] Hossein, M., Ripanda, A. S. (2025): Pollution by antimicrobials and antibiotic resistance genes in East Africa: Occurrence, sources, and potential environmental implications. – Toxicology Reports 14: 101969. https://doi.org/10.1016/j.toxrep.2025.101969.

[9] Jiang, B., Wang, T., Li, F., Li, D., Yang, Y., Yu, H., Dong, X. (2023): Polyoxometalate as pivotal interface in SnO_2@PW_{12}@TiO_2 coaxial nanofibers: From heterojunction design to photocatalytic and gas sensing applications. – Sensors and Actuators B: Chemical 390: 133928. https://doi.org/10.1016/j.snb.2023.133928.

[10] Li, Y., Wang, J., Lin, C., Lian, M., He, M., Liu, X., Ouyang, W. (2024): Occurrence, removal efficiency, and emission of antibiotics in the sewage treatment plants of a low-urbanized basin in China and their impact on the receiving water. – Science of The Total Environment 921: 171134. https://doi.org/10.1016/j.scitotenv.2024.171134.

[11] Lu, N., Lu, Y., Liu, F., Zhao, K., Yuan, X., Zhao, Y., Li, Y., Qin, H., Zhu, J. (2013): H3PW12O40/TiO2 catalyst-induced photodegradation of bisphenol A (BPA): Kinetics, toxicity and degradation pathways. – Chemosphere 91(9): 1266-1272. https://doi.org/10.1016/j.chemosphere.2013.02.023.

[12] Ma, J., Zhu, C., Xu, Y., Lu, J., Huang, L., Yang, Z. (2017): Photocatalytic degradation of gaseous benzene with $H_3PW_{12}O_{40}/TiO_2$/palygorskite composite catalyst. – Journal of Saudi Chemical Society 21(2): 132-142. https://doi.org/10.1016/j.jscs.2015.02.001.

[13] Maharathi, P., Lo, S. (2025): Facile synthesis of 2D "GO"-TiO_2 @biochar hybrid nanocomposites for synergistic adsorption and photocatalytic elimination of veterinary antibiotics from livestock effluents. – Chemical Engineering Journal 521: 166205. https://doi.org/10.1016/j.cej.2025.166205.

[14] Moreno Orea, J. E., Gracia, Y., Jiménez, J. M., Silva González, N. R., Sabinas Hernández, S. A., Kuri, U. S. (2025): Variation of Anatase and Rutile Concentrations in TiO2 Electrospun Fibers via Precursor Solution Modification. – Journal of Physics and Chemistry of Solids 208: 113028. https://doi.org/10.1016/j.jpcs.2025.113028.

[15] Nugraha, M. W., Kim, S., Roddick, F., Xie, Z., Fan, L. (2025): A review of the recent advancements in adsorption technology for removing antibiotics from hospital wastewater. – Journal of Water Process Engineering 70: 106960. https://doi.org/10.1016/j.jwpe.2025.106960.

[16] O'Byrne, M., Kerzabi, B., Abbarchi, M., Lifschitz, A., Zamora, T., Malgras, V., Gourdin, A., Modaresialam, M., Grosso, D., Putero, M. (2024): Investigation of the anatase-to-rutile transition for TiO2 sol-gel coatings with refractive index up to 2.7. – Thin Solid Films 790: 140193. https://doi.org/10.1016/j.tsf.2023.140193.

http://www.aloki.hu ● ISSN 1589 1623 (Print) ● ISSN1785 0037 (Online)
DOI: http://dx.doi.org/10.15666/aeer/2401_395407

[17] Peng, T., Song, B., Wang, Y., Yuan, J., Yang, Z., Tang, L. (2025): Trophic transfer of sulfonamide antibiotics in aquatic food chains: A comprehensive review with a focus on environmental health risks. – Environmental Pollution 369: 125823. https://doi.org/10.1016/j.envpol.2025.125823.

[18] Shang, M., Dong, J., Xie, H., Li, Y., Wan, N., Xiong, Z., Lai, X. (2025): Unraveling transport mechanisms and rainfall event-driven controls on non-point source antibiotic pollution by high-resolution process-based modeling. – Journal of Hazardous Materials 495: 139177. https://doi.org/10.1016/j.jhazmat.2025.139177.

[19] Sinha, R., Ghosal, P. S. (2023): A comprehensive appraisal on status and management of remediation of DBPs by TiO2 based-photocatalysts: Insights of technology, performance and energy efficiency. – Journal of Environmental Management 328: 117011. https://doi.org/10.1016/j.jenvman.2022.117011.

[20] Su, Z., Wen, D., Gu, A. Z., Zheng, Y., Tang, Y., Chen, L. (2023): Industrial effluents boosted antibiotic resistome risk in coastal environments. – Environment International 171: 107714. https://doi.org/10.1016/j.envint.2022.107714.

[21] Synowiec, M., Radecka, M., Micek-Ilnicka, A. (2023): UV light enhanced catalytic performance of heteropolyacid-TiO_2 systems. – Journal of Catalysis 417: 481-496. https://doi.org/10.1016/j.jcat.2022.12.028.

[22] Wu, Y., Zhang, J., Xiao, L., Chen, F. (2009): Preparation and characterization of TiO2 photocatalysts by Fe3+ doping together with Au deposition for the degradation of organic pollutants. – Applied Catalysis B: Environmental 88(3-4): 525-532. https://doi.org/10.1016/j.apcatb.2008.10.008.

[23] Wu, D., Bai, H., He, L., He, L., Gao, F., Liu, C., Van den Brink, P. J., Smidt, H., Ying, G. (2025): From river to groundwater: Antibiotics pollution, resistance prevalence, and source tracking. – Environment International 196: 109305. https://doi.org/10.1016/j.envint.2025.109305.

[24] Yin, S., Wang, T., Pei, W., Yang, Y., Tao, H., Li, D., Yu, H., Yu, W., Dong, X. (2024): Synergy of oxygen vacancy and electron donor in one-dimensional black TiO2/phosphotungstic acid with Z-scheme heterojunctions for enhanced photocatalytic CO_2 reduction. – Journal of Environmental Chemical Engineering 12(6): 115001. https://doi.org/10.1016/j.jece.2024.115001.

[25] Zhang, L., Han, Y., Yang, J., Deng, S., Wang, B. (2021): Construction and photocatalysis of carbon quantum dots/layered mesoporous titanium dioxide (CQDs/LM-TiO2) composites. – Applied Surface Science 546: 149089. https://doi.org/10.1016/j.apsusc.2021.149089.

http://www.aloki.hu ● ISSN 1589 1623 (Print) ● ISSN1785 0037 (Online)
DOI: http://dx.doi.org/10.15666/aeer/2401_395407